PROCEEDINGS OF SCIENCE

Hadronic vacuum polarization from step scaling in the Schwinger model

Fabian Justus Frech[a,*] **for the Budapest-Marseille-Wuppertal Collaboration**

[a] *Bergische Universität Wuppertal,*
Gaussstraße 20, Wuppertal, Germany

E-mail: frech@uni-wuppertal.de

We compute the quark-connected part of the hadronic vacuum polarization function (HVP) in the Schwinger Model. We develop a new strategy, similar to the well-known step-scaling, to compute the HVP in a large range of the energy scale. Additionally we use the HVP and the Wilson flow to determine the line of constant physics. The strategy developed here can be useful to compute the hadronic contribution to the running of the electromagnetic coupling in dynamical QCD up to the scale of the mass of the Z boson.

The 38th International Symposium on Lattice Field Theory, LATTICE2021 26th-30th July, 2021
Zoom/Gather@Massachusetts Institute of Technology

*Speaker

PoS(LATTICE2021)218

1. Introduction

It is common knowledge that the QED coupling has an energy dependence with some of its contributions originating from hadrons. These contributions can be computed using lattice QCD. This paper deals with a method calculating these contributions up to the energy scale of the Z boson mass.

Here we propose a strategy to compute the hadronic vacuum polarization function (HVP) over two orders of magnitude in the energy. Our procedure is very similar to the well known step scaling technique, and is based on the discrete Adler function. We use the Schwinger model (QED_2) to test this strategy.

An important ingredient for this computation is the line of constant physics (LCP), which in principle has to be determined first. Along the LCP we can then compute the HVP. Here we proceed the other way around. In Section 2 we present the computation of the HVP using the analytic result for the LCP, which is a well known function in QED_2. In Section 3 we turn to the determination of the LCP, where we can compare the result of our procedure to the analytic formula.

2. Hadronic vacuum polarization

The HVP can be obtained from the Fourier transform of the coordinate space current-current correlator $c_{\mu\nu}(t,x)$ as:

$$\Pi(Q) = \frac{1}{2Q^2} \sum_{t,x=-L/2}^{L/2} e^{iQ(t+x)} \left(c_{tt}(t,x) - c_{tx}(t,x) - c_{xt}(t,x) + c_{xx}(t,x)\right) \tag{1}$$

Computing the difference in the vacuum polarization between two largely separated momenta Q_0 and Q_n poses a serious difficulty, since in practice a single lattice cannot accommodate both scales. Instead we proceed in the following way: assuming that there is an $n > 0$ integer such that $Q_n = 2^n Q_0$ we can compute the difference as the following telescoping sum:

$$\Pi(Q_\mathrm{n}) - \Pi(Q_0) = \Delta(2^{n-1}Q_0) + \Delta(2^{n-2}Q_0) + \cdots + \Delta(Q_0)\ , \tag{2}$$

where we introduced the discrete Adler function

$$\Delta(Q) = \Pi(2Q) - \Pi(Q)\ . \tag{3}$$

This is our primary observable. The central idea of our strategy is that we utilize different physical volumes for the different terms in Equation (2). We expect on general grounds that larger energies are less sensitive to the volume and can therefore be computed in smaller volumes without increasing the finite volume effects. This makes the calculation feasible in terms of computer time. During each step we perform simulations with several lattice spacings to be able to perform a continuum extrapolation. For the analysis of finite size effects we compare the results of the different steps at the same physical momentum.

We test the procedure in QED_2, for which we make simulations with $n = 6$ steps, thus covering factor $2^7 = 128$ change in the energy scale. This range is about the same that one has between the energy scales of typical lattice QCD computations and the mass of the Z boson. We use Symanzik

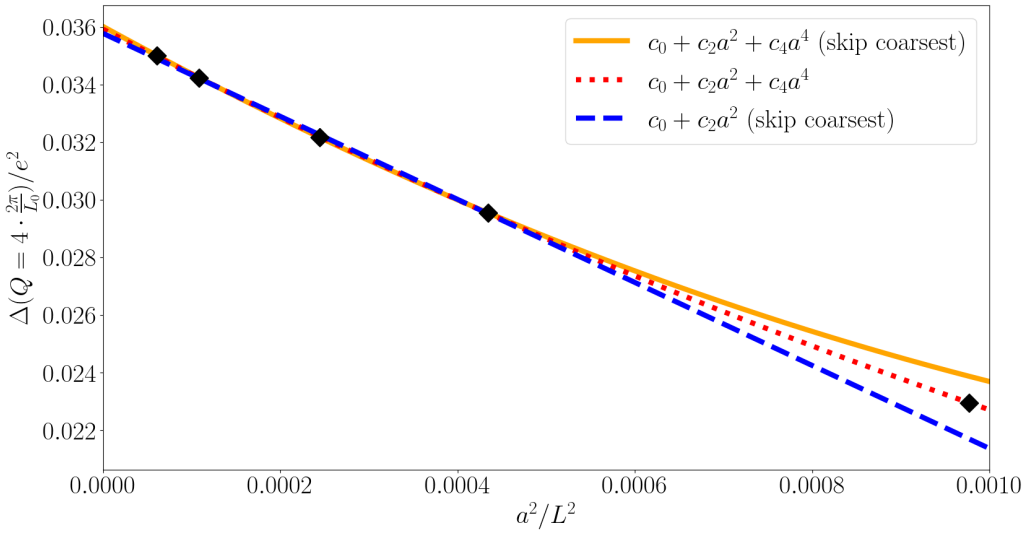

Figure 1: The continuum extrapolation of the Adler function at the fourth lattice momentum in the zeroth step. Different lines correspond to different continuum extrapolations: one quadratic in a^2 (dotted), one quadratic in a^2 skipping the coarsest lattice (solid) and one linear in a skipping the coarsest lattice (dashed).

improved gauge action with a gauge coupling parameter e and we use the notation $\beta = \frac{1}{e^2}$ later on. We set the mass of the fermions as $\beta m^2 = 0.8$, which is a dimensionless and scale independent quantity in QED_2. In the zeroth step we fix the volume by setting $mL_0 = 16$ and in the further steps we decrease the physical extension by a factor of two, i.e. $mL_n = 16/2^n$. The gauge configurations are generated with a Metropolis algorithm with an additional update step to improve the tunneling of the topology [1, 2] . We use two flavors of dynamical staggered fermions, whose effect on the gauge configuration is included by reweighting with the fermion determinant.

In each step we perform continuum extrapolation using lattices with lattice extent $L/a \in \{32, 48, 64, 96, 128\}$. We set the β-parameter proportional to $\frac{1}{a^2}$ and the mass parameter proportional to a. We work with several different momentum values of the Adler function on each lattice. The small momenta exhibit small lattice artifacts but large finite volume effects, while the larger momenta behave the opposite way. We find a good compromise between these effects at the fourth lattice momentum $Q = 4 \cdot \frac{2\pi}{L}$. The continuum extrapolation in the zeroth step can be seen on Figure 1. We estimate systematic errors by making continuum extrapolations with functions with different lattice spacing dependence. We include these different values into a histogram whose width gives the systematic error [3].

Also finite volume effects have to be considered. The fourth lattice momentum in step n is the same physical momentum as the second one in step $n + 1$ and the first one in step $n + 2$. Thus we can perform a finite volume analysis using the finest lattice ($L/a = 128$) from step n, the third finest ($L/a = 64$) from step $n + 1$ and the coarsest ($L/a = 32$) from step $n + 2$. We assume finite volume effects can be described by the function $\exp(-M_\pi L)$, where M_π is the mass of the pseudo-scalar meson. The corresponding fits can be seen in Figure 2. The extrapolation shows that the relative deviation of the fourth lattice momentum from the infinite volume limit is always smaller than

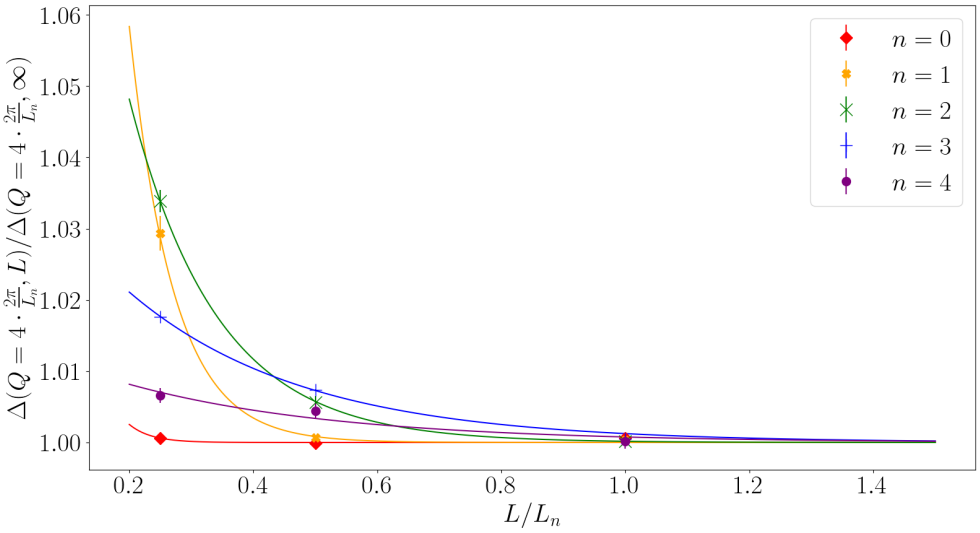

Figure 2: The infinite volume extrapolation of the discrete Adler function in different steps of our procedure. The curves are constant plus $\exp(-M_\pi L)$ type fits. The errors are statistical.

0.05 %. Thus by using the fourth lattice momentum in each step we can assume finite volume effects on the level of half a per-mill in the final results.

Our final results for the discrete Adler function can be seen in Figure 3. The black line in Figure 3 is the one-loop perturbative result [4]:

$$\Pi(Q)_{1-\text{loop}}/e^2 = \frac{1}{\pi}\frac{1}{Q^2}\left(1 + \frac{2m^2}{Q^2}\frac{1}{R}\log\frac{1+R}{1-R}\right) \tag{4}$$

with $R = \sqrt{1 - \frac{4m^2}{Q^2}}$. Note, that this expression has an analytical continuation to $Q \leq 2m$, that we use here. For large energies it matches our simulations well, however for small energies it deviates significantly, the reason of which are effects beyond one-loop perturbation theory. We checked this by performing simulations with different m^2/e^2 at the momentum $Q = 4 \cdot \frac{2\pi}{L_0}$, and found that in the limit $e^2/m^2 \to 0$ the simulation result converges to the one-loop perturbative value. Our

Q/e	$\Delta(Q)/e^2$	stat.	disc.	fin. vol.	total
1.405	0.036013	0.06 %	0.04 %	0.05 %	0.09 %
2.810	0.019360	0.01 %	0.03 %	0.03 %	0.05 %
5.620	0.006515	0.01 %	0.03 %	0.02 %	0.04 %
11.240	0.001806	0.01 %	0.05 %	0.05 %	0.07 %
22.480	0.000467	0.02 %	0.03 %	0.02 %	0.04 %
44.960	0.000118	0.01 %	0.02 %	0.05 %	0.05 %
89.920	0.000029	0.01 %	0.02 %	0.05 %	0.05 %

Table 1: The continuum limit of the Adler function measured on the fourth momentum on each step.

continuum and infinite volume extrapolated results for the seven steps are given in Table 1. Adding

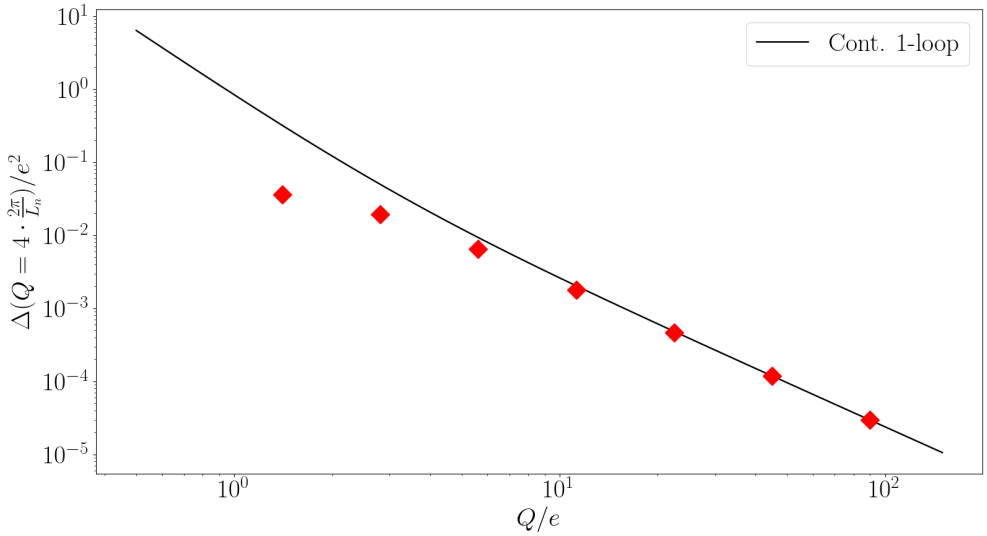

Figure 3: The seven points show the discrete Adler function measured in seven different steps. The combined statistical and systematic error is smaller than the symbol size. The black line is the one-loop perturbative prediction [4].

up the values gives the final result:

$$\Pi(2^7 Q_0) - \Pi(Q_0) = 0.064308(23)_{\text{stat.}}(76)_{\text{syst.}} \,, \tag{5}$$

where the first error is statistical, the second is the quadratic sum of the systematic errors of our extrapolations. We reach a total accuracy of 0.12%.

3. Line of constant physics

Here we develop a strategy to compute the LCP for the steps (i.e. the lattices of a fixed volume) given in the previous chapter assuming that in the initial step the LCP is already known. For a D dimensional parameter space one needs D different observables to define the LCP. It is useful to choose them in such a way, that the observables are sufficiently sensitive to variation of the parameters.

3.1 General strategy

The method which is used here to set the LCP is called step scaling [5] [6]. It is applied in the following way: we consider N lattices of the same physical volume but with different lattice spacings. The LCP is already known for the K coarsest lattices of this set. The observables, which define the LCP, are computed on the K coarsest lattices, so one can extrapolate their expectation values to finer lattice spacings. At the same time we perform simulations on the $N-K$ finer lattices, at each of which we choose at least $D+1$ different parameters. From the observables measured at these different parameters we construct interpolating functions. The point in the parameter space, where the interpolations match the extrapolations from the coarser lattices gives the LCP. We apply

this procedure for all the $N - K$ lattice spacings. An example with $N = 5$, $K = 4$ and $D = 1$ can be seen in Figure 4.

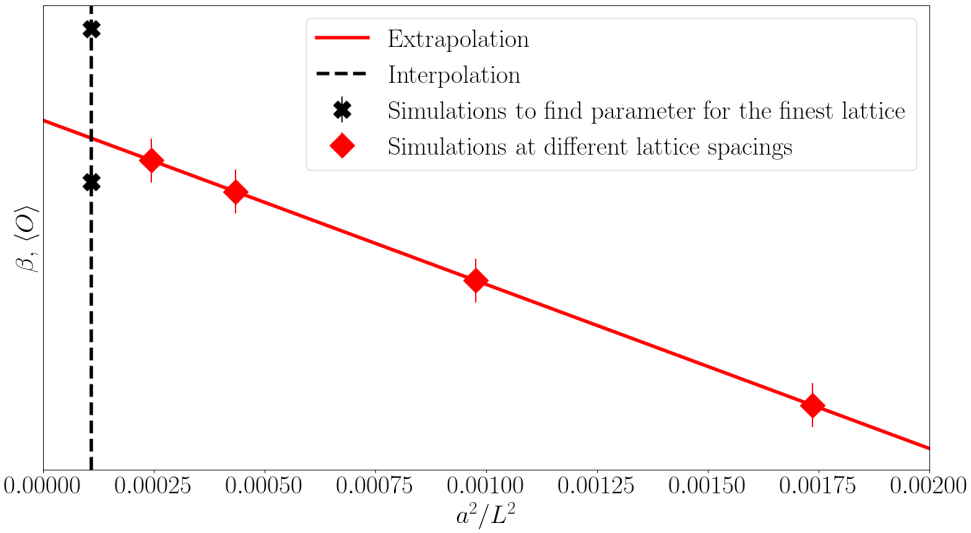

Figure 4: Illustration of the step scaling procedure. The inverse coupling parameter β is set using an observable $\langle O \rangle$. The solid line shows the extrapolation of $\langle O \rangle$ to finer lattices. The dashed line shows the interpolation of $\langle O \rangle$ at the finer lattice. The point, in which the solid line hits the dashed one gives our estimation for β.

The increasing computational costs prevent us from going to very fine lattices we would like to simulate. Thus in each step we decrease the physical extent by a factor $\alpha < 1$. At the same time we switch to new observables, that are less sensitive to finite volume effects. We can then perform the previously mentioned procedure again.

3.2 Estimation of uncertainties

Obviously we have to associate statistical and systematical uncertainties to the procedure described in Section 3.1. Systematical uncertainties mainly originate from the extrapolations to finer lattice spacings. To consider these uncertainties one uses $(F_i)_{i=1,\dots,D}$ different extrapolating functions. Thus there are $\prod_{i=1}^{D} F_i$ proposals for the $(N - K) \times D$ parameters estimated in this step. Each of this proposals is weighted with the product of the Akaike Information Criterions (AIC) of the fit used for the considered proposal. The AIC of one extrapolation is given by:

$$\exp\left(-\frac{1}{2}(\chi^2 + 2n_f - n_p)\right) , \tag{6}$$

where n_f is the number of fit parameters of the extrapolation and n_p is the number of points that are used in the fit [3]. We now randomly choose I of those proposals and use them as parameters in the next step. Since the parameters of different samples do not differ that much we can just perform 2^D different simulations for each lattice spacing and perform linear interpolations to compute the observables at each parameter set. In this step we make $I \times \prod_{i=1}^{D} F_i$ proposals. From these we choose

I representatives for the next step. For the different sets of parameters we use flat weighting instead of the AIC. The computation of the statistical uncertainties is somewhat simpler: the observables of each simulation are put in N_J Jackknife samples. Then the whole step scaling procedure is performed N_J times, the AIC is always computed on the full sample.

3.3 Application and test of the strategy in QED_2

We apply the strategy described in Section 3.1 in QED_2. Since we have exact formulas for the LCP, we can investigate the quality of our procedure. The line of constant physics is described by two parameters: the inverse squared gauge coupling β and the fermion mass m, so we have $D = 2$.

The observable sensitive to β is chosen to be a certain time along the Wilson flow [7]. The flow is computed with a fourth order Runge-Kutta algorithm to solve the following partial differential equation:

$$\frac{d}{d\tau}U_\tau(x,\mu) = -\left[\partial_{x,\mu}\frac{1}{\beta}S(U_\tau)\right]U_\tau(x,\mu) \tag{7}$$

where $S(U)$ is the gauge action. We define our observable to be the time τ_0 at which $\tau S(U_\tau)/(L/a)^2$ takes the value $0.375 \cdot 4^{-n}$. By introducing a factor 4^{-n} in the nth step of our procedure, we make sure that the finite size effects on τ_0 remain small as the physical volume is decreased.

It seems obvious to use the pseudo-scalar meson mass to set the fermion mass since it has a strong fermion mass dependence. Unfortunately at higher steps the physical extension of the lattices becomes small such that the meson does not fit into the box anymore. Thus we use a certain value of the discrete Adler function instead. This observable has the advantage that the momentum increases according to the decreasing of the volume. Thus it can be resolved in any step. The disadvantage of this observable is, that it only has a strong mass dependence if the fermion mass and Q are at the same order of magnitude [4]. So we multiply the mass of the valence quarks in the nth step by 2^n. This multiplication is justified, because staggered fermions have no additive mass renormalization.

We set $N = 6$, $K = 4$ and $\alpha = \frac{1}{2}$. We use $N_J = 48$ Jackknife samples and set I to 30. For both the extrapolation of the Adler function and the Wilson flow time we use 3 different interpolations in a^2 (quadratic and linear through all points and an additional linear leaving out the coarsest one.). The Adler function in each step is evaluated at $Q = 4 \cdot \frac{2\pi}{L_n}$, where $L_n = 2^{-n}L_0$ is again the physical lattice extension in the nth step.

We start in the zeroth step with the same volume and the exact LCP as in Section 2. An additional coarse lattice ($L/a = 24$) is added to have four lattice spacings for the extrapolations. In each step we use the LCP from the previous step on lattices $L/a \in \{24, 32, 48, 64\}$, perform continuum extrapolations, and determine the new LCP on lattices $L/a \in \{96, 128\}$. The results of five steps of this procedure can be seen in Figure 5. The LCP computed by the step-scaling procedure agrees with the analytical solution within our combined statistical and systematic error. The deviation of the parameters is of order of half a percent. The statistical error is dominant and the relative uncertainty grows with increasing step number.

3.4 Impact on the precision of the Adler function

Here we investigate how uncertainties on the LCP propagate into the Adler function (Section 2). Let us start with the one originating from the β-uncertainty. From the point at which the parameter

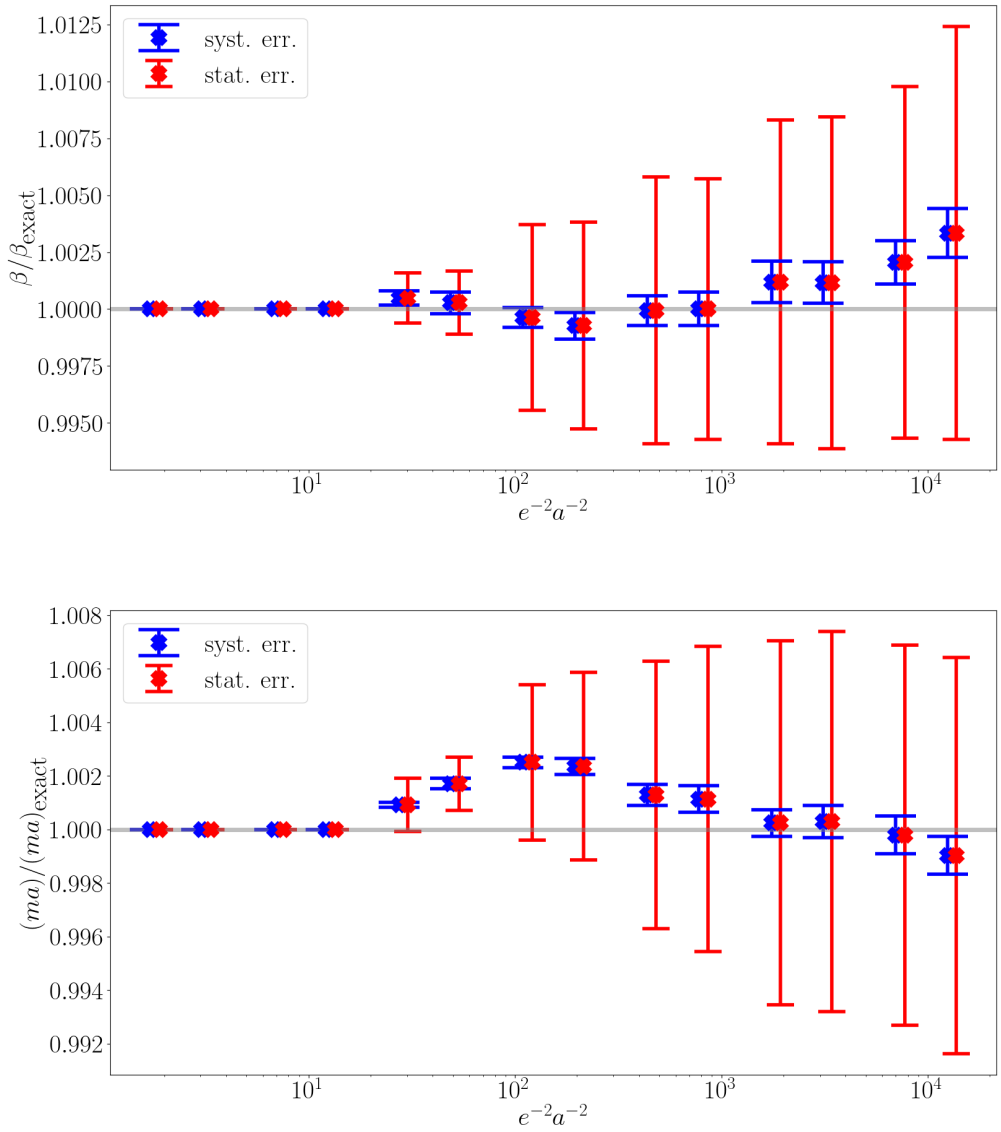

Figure 5: The relative deviation of the lattice spacing (top panel) and the mass parameter (bottom panel) compared to the exact value. The systematic errors include discretization effects as well as accumulated uncertainties from the previous steps.

starts to deviate due to the step scaling, the discrete Adler function is proportional to $\frac{1}{Q^2} \propto \frac{1}{\beta}$ (Figure 3). So if the estimated value of β is given by $(1 \pm \epsilon)\beta_{\text{exact}}$ the relative deviation of the Adler function is given by $\mp\epsilon$. The relative deviation of β increases from 0.1 % in the first step to 0.9 % in the last step. So we estimate, using the fact that the contribution of the first steps is stronger, a total deviation of 0.25 % of the HVP. In Figure 6 one can see the relative derivative of the discrete Adler function with respect to the mass. It is estimated via the secant slope through m and $1.05m$. For small volumes resp. high energies this derivative is close to zero. In the region which dominates the

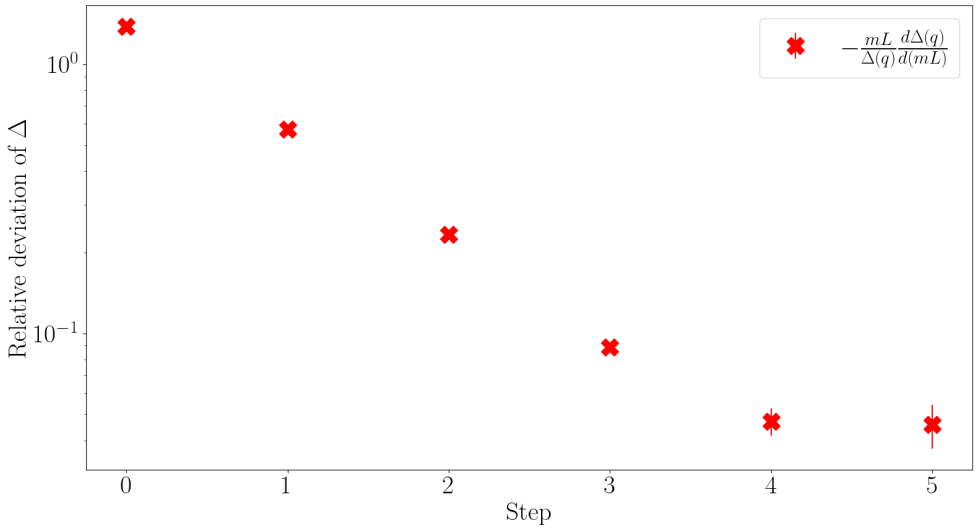

Figure 6: The continuum extrapolated normalized mass derivative of the Adler function evaluated at the fourth momentum on six different volumes.

value for $\Pi(2Q_n) - \Pi(Q_0)$ the relative derivative is between 10 and 100 percent of the relative mass deviation, which is between 0.1 % and 0.5 % in this region. The total uncertainty originating from the mass deviation is then given by 0.15 %. Thus assuming we had calculated the HVP with the step scaling parameters we have additional uncertainties of 0.000155 (β deviation) and 0.000095 (mass parameter deviation). All in all the parameter uncertainties dominate the other error sources from Section 2.

4. Conclusion and outlook

First we calculated the hadronic vacuum polarization function in QED_2 including continuum and finite volume extrapolations, and reached a precision of one per-mill. Secondly we constructed a step scaling strategy to compute the line of constant physics. This method was also tested in QED_2 and it was shown that it gives reliable results. Finally we estimated the uncertainty of the measurement of the HVP under the assumption that the LCP was set with the step scaling procedure. We found that the uncertainty was smaller than 0.3 % in this case.

Our method can also be applied to compute the hadronic vacuum polarization in QCD. A major difference is, that whereas in QED_2 the discrete Adler function decreases for large energies, in QCD it approaches to a finite value. Thus the high energy range makes a larger contribution to the final result.

References

[1] S. Dürr, *Physics of η' with rooted staggered quarks*, *Phys. Rev. D* **85** (2012) 114503.

[2] T. Eichhorn and C. Hoelbling, *Comparison of topology changing update algorithms*, 2112.05188.

[3] S. Borsanyi, Z. Fodor, J.N. Guenther, C. Hoelbling, S.D. Katz, L. Lellouch et al., *Leading hadronic contribution to the muon magnetic moment from lattice qcd*, *Nature* **593** (2021) 51–55.

[4] C. Adam, R. Bertlmann and P. Hofer, *Overview on the anomaly and schwinger term in two-dimensional qed*, *Riv. Nuovo Cim. 16, 1–52 (1993)* (2007) .

[5] R. Sommer and U. Wolff, *Non-perturbative computation of the strong coupling constant on the lattice*, 1501.01861.

[6] M. Lüscher, P. Weisz and U. Wolff, *A numerical method to compute the running coupling in asymptotically free theories*, *Nuclear Physics B* **359** (1991) 221.

[7] M. Lüscher, *Properties and uses of the wilson flow in lattice qcd*, *Journal of High Energy Physics* **2010** (2010) .